Microstructural characterization of Inconel 713C superalloy after creep testing

Charakterystyka mikrostruktury nadstopu Inconel 713C po badaniach pełzania

Małgorzata Grudzień[1]*, Rafał Cygan[2], Zenon Pirowski[1], Łukasz Rakoczy[3]

[1]*Foundry Research Institute, ul. Zakopianska 73, 30-418 Krakow, Poland*

[2]*Consolidated Precision Products, Investment Casting Division CPP-Poland, ul. Hetmanska 120, 35-078 Rzeszow, Poland*

[3]*AGH – University of Science and Technology, Faculty of Metals Engineering and Industrial Computer Science, Department of Physical and Powder Metallurgy, al. A. Mickiewicza 30, 30-059 Krakow, Poland*

[1]*Instytut Odlewnictwa, ul. Zakopiańska 73, 30-418 Kraków, Polska*

[2]*Consolidated Precision Products, Investment Casting Division CPP-Poland, ul. Hetmańska 120, 35-078 Rzeszów, Polska*

[3]*AGH Akademia Górniczo-Hutnicza im. S. Staszica w Krakowie, Wydział Inżynierii Metali i Informatyki Przemysłowej, Katedra Metaloznawstwa i Metalurgii Proszków, al. A. Mickiewicza 30, 30-059 Kraków, Polska*

*Corresponding author: malgorzata.grudzien@iod.krakow.pl

Abstract

The main aim of this investigation was to determine the microstructural degradation of Inconel 713C superalloy during creep at high homologous temperature. The alloy in as cast condition was characterized by large microstructural heterogeneity. Inside equiaxed grains dendrite cores consisted of γ' precipitates surrounded by channels of matrix, whereas enrichment of interdendritic spaces in carbide formers, Zr and B resulted in the formation of additional constituents, namely M_3B_2, Ni_7Zr_2 and eutectic island γ/γ'. Directional coarsening of γ' precipitates (rafting) under applied stress and decomposition of primary MC-type carbides accompanied by the formation of secondary carbides enriched in Cr and γ' phase was observed.

Keywords: degradation, Inconel 713C, NbC, $M_{23}C_6$

Streszczenie

Głównym celem badania było określenie degradacji mikrostruktury nadstopu Inconel 713C zachodzącej podczas badania pełzania w wysokiej temperaturze homologicznej. Badany nadstop bezpośrednio w stanie lanym charakteryzuje się wysoką niejednorodnością mikrostrukturalną. Wewnątrz ziaren równoosiowych rdzenie dendrytów składają się z wydzieleń γ' otoczonych kanałami osnowy, natomiast wzbogacenie przestrzeni międzydendrytycznych w pierwiastki węglikotwórcze, a także Zr i B, prowadzi do tworzenia dodatkowych składników, mianowicie eutektyki γ/γ', węglików MC, borków M_3B_2 oraz fazy międzymetalicznej Ni_7Zr_2. W trakcie pełzania przy parametrach T = 982°C i naprężeniu σ = 152 MPa zaobserwowano rafting typu N fazy międzymetalicznej γ'. W przestrzeniach międzydendrytycznych w wyniku częściowego rozpuszczenia węglików typu MC wydzieliły się węgliki $M_{23}C_6$ bogate w Cr.

Słowa kluczowe: degradacja, Inconel 713C, NbC, $M_{23}C_6$

1. Introduction

Inconel 713C belongs to the group of nickel-based superalloys, strengthened primaly by the high volume fraction of intermetallic γ' phase, present to above 1000°C. Very good castability, creep resistance and microstructural stability make these superalloys suitable for manufacture of a low-pressure turbine (LPT) guide vanes in turbo-fan engines [1−4]. Polycrystalline turbine blades are typically manufactured by investment casting process known as the lost-wax process. These complex castings must meet all the extremely strict aerospace quality requirements. Ni-based superalloys are characterized by the ability of stressed γ' precipitates to transformation into plates at the high temperature and normal to the axis of the applied stresses (Fig. 1). The phenomenon of a directional growth (coarsening) is usually called "rafting" [5,6], while N-type behaviour is associated with negative misfit alloys stressed in tension.
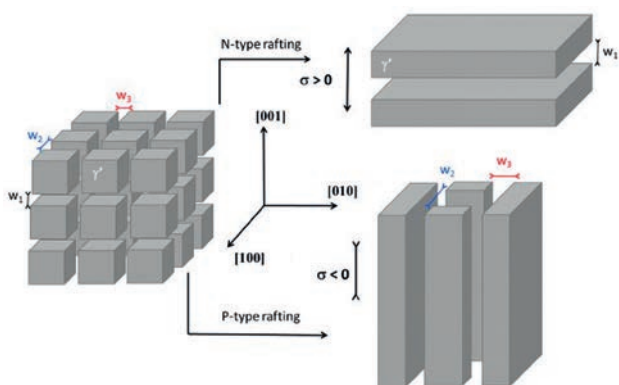

Fig. 1. Scheme of N- and P-type rafting in superalloys strengthened by cubic-shaped γ' precipitates [5]
Rys. 1. Rafting typu N oraz P w nadstopach niklu umacnianych fazą międzymetaliczną γ' [5]

Lattice misfit is defined as:

$$\delta = 2(a_{\gamma'} - a_\gamma)/(a_{\gamma'} + a_\gamma),$$

where $a_{\gamma'}$ and a_γ are the lattice constant of the γ' phase and γ matrix respectively. During exposure to high temperature formation of continuous grain boundary carbide network, TCP phases and MC carbide degeneration can also occur. Most of these features are detrimental to properties of material such as tensile strength and creep resistance [7−10]. Usually, the nickel-based superalloys are heat treated (solution + ageing). However, Inconel 713C achieves sufficiently high strength directly in the casting in the as cast condition [11−13]. According to the AMS5391 the minimum time to rupture during creep of as cast Inconel 713C at 1800°F (~980°C) under 22 psi (~152 MPa) is 30 hours [14]. The tests are carried out at a temperature which significantly exceeds the in-service

requirements of the Inconel 713C castings. To achieve the highest properties demand intensive research and testing in order to make correlations between mechanical properties and manufacturing parameters including the composition of shell mould. The aim of this work is to show all details about the parameters of investment casting and creep resistance at high homologous temperature under low stress with particular emphasis on change of primary (as cast) microstructure of Inconel 713C.

2. Experimental procedure

Inconel 713C was provided by Canon Muskegon Company in the form of bar. Results of chemical composition obtained by optical emission spectroscopy (OES) are shown in Table 1. The wax pattern, similar in shape and dimensions to the required tensile specimen (Fig. 2) was injection moulded, and then a ceramic monolithic mould was built up around this pattern by a series of dip coatings. The casting was made in the Investment Casting Division of CPP Corp. Poland in Rzeszow and all technological conditions were as similar as possible to company standards. The prime coating of shell mould consisted of zircon filler, colloidal silica binder and 5% of cobalt aluminate ($CoAl_2O_4$). Alumina grit was used as a primary stucco, and then several coats of ceramic slurries based on alumina silicate powders and colloidal silica binder and as a backup stucco aluminate silicate grit were applied. Master heat charge was melted in a zirconia crucible mounted in the vacuum Consarc furnace. During melting and subsequent pouring level of vacuum was 2×10^{-3} mbar. The liquid metal at 1520°C was poured into a preheated (1000°C) mould. After the alloy has solidified and cooled, the mould was broken and then casting was cut out from the assembly. To obtain the required dimensions of the test specimen (Fig. 2) with optimal surface roughness and dimensions final machining was carried out. Creep resistance test was carried out in accordance with the requirements of ASTM E139 standard using the Walter + Bai AG LFMZ-30 device at temperature 982°C and stress 152 MPa.

Metallographic observations were preceded by standard metallographic preparation and chemical etching in 50 ml lactic acid, 30 ml nitric acid, 2 ml hydrofluoric acid: AG21. The observations at higher magnification before and after creep was carried out by light microscopy (LM) and scanning electron microscopy (SEM). For SEM, samples were etched in 50 ml water, 50 ml hydrochloric acid, 50 ml nitric acid, 1.5 g molybdic acid: no. 17 Etch (micro) reagent. Image analysis was used to calculate the number of equiaxed grains, mean area, mean perimeter, and number of precipitates per mm^2. For imaging and EDS analyses, a 15 kV accelerating voltage was used.

Table 1. Chemical composition of Inconel 713C
Tabela 1. Skład chemiczny stopu Inconel 713C

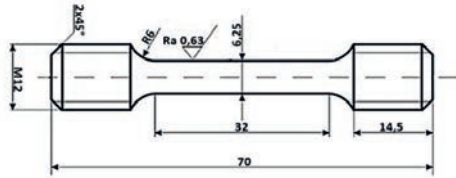| Element	Cr	Al	Mo	Nb	Ti	C	Zr	Co	B	S	P	Ni
% wt.	14.24	5.93	4.29	2.45	0.92	0.11	0.08	0.04	0.012	0.003	0.004	Bal.

Fig. 2. Geometry and dimensions of the specimen for creep test (mm)
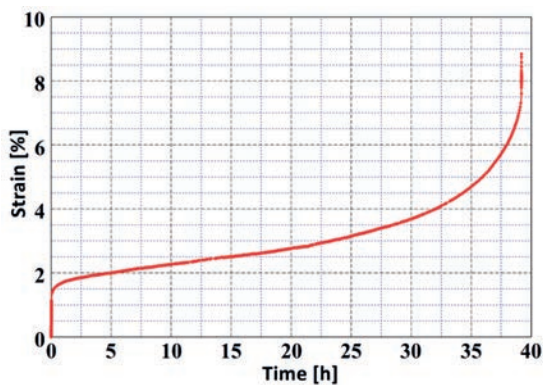*Rys. 2. Geometria próbki do badań pełzania (mm)*

3. Results and discussion

Fig. 3. Creep curve of Inconel 713C
Rys. 3. Krzywa pełzania nadstopu Inconel 713C

At high temperature/low stress (982°C/152 MPa), Inconel 713C showed short-term primary stage and then steady state creep (0.057875% per h) and finally pronounced strain appearing at the tertiary stage (Fig. 3). Creep curve had the classical shape, while the time to rupture was almost 40 h, in accord with AMS5391 requirement of minimum 30 h. The macrostructure of Inconel 713C after binarization consisting of 18 equiaxed grains is shown in Figure 4. The generally unacceptable chill zone structure of the inner surface of casting was not present. The stereological parameters, presented in Table 2, indicate that relatively fine-grain structure was obtained. The mean area of detected grains was 4.08 mm², while the perimeter exceeded 20 mm. Standard deviations were relatively high due to irregular grains size and local condition of solidification process. Pouring temperature was relatively high, and so only 0.23 grain are per mm² was observed. The grain size in cast superalloys depends mainly on the velocity of

growth and nucleation rate. The obtained structure was caused by the reaction between the Cr, Al and Ti consisted in Inconel 713C and cobalt aluminate (primary coat). Cobalt in the compound is displaced by these elements to form Co fine particles, which are considered to be the nucleants during solidification of casting [12].
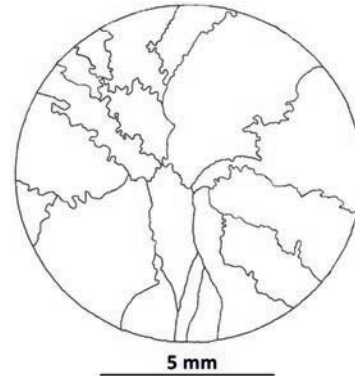

Fig. 4. Binary image of Inconel 713C macrostructure
Rys. 4. Obraz binarny makrostruktury Inconel 713C

Table 2. Stereological parameters of Inconel 713C casting
Tabela 2. Parametry stereologiczne nadstopu Inconel 713C

	Number of grains	Mean area, mm²	Mean perimeter, mm	Number of perimeter per mm²
Value	18	4.08	20.48	0.23
Standard deviation		3.56	9.39	

The microstructure of as-cast Inconel 713C before mechanical testing at elevated temperature is shown in Figure 5. Dissimilarity between of dendrite core and interdendritic spaces microstructure originated from the change of solubility of alloying elements in γ-matrix during solidification and cooling (Fig. 5a). Dendrite cores consist of cubic-shaped γ' precipitates surrounded by γ channels, while interdendritic spaces were strongly enriched in Nb, Zr and B which led to the creation of NbC (Fig. 5b), M_3B_2 (Fig. 5c) and Ni_7Z_2 (Fig. 5d) in the close vicinities of eutectic islands. More primary microstructure detail were presented in [15]. Fractographic observations revealed intergranular cracking with numerous faults resulting from the orientation of equiaxed grains (Fig. 6a). Cracks formed during creep were also observed inside the sample, which indicates a local weakening of grain boundaries (Fig. 6b). These crack length were of several dozen micrometers, less often more than 100 μm. In Figure 7 SEM micrograph of crept Inconel 713C is presented. A change in morphology, from the undeformed structure, of strengthening phases both in dendrite core and interdendritic spaces was evident. Inconel 713C is characterized by the
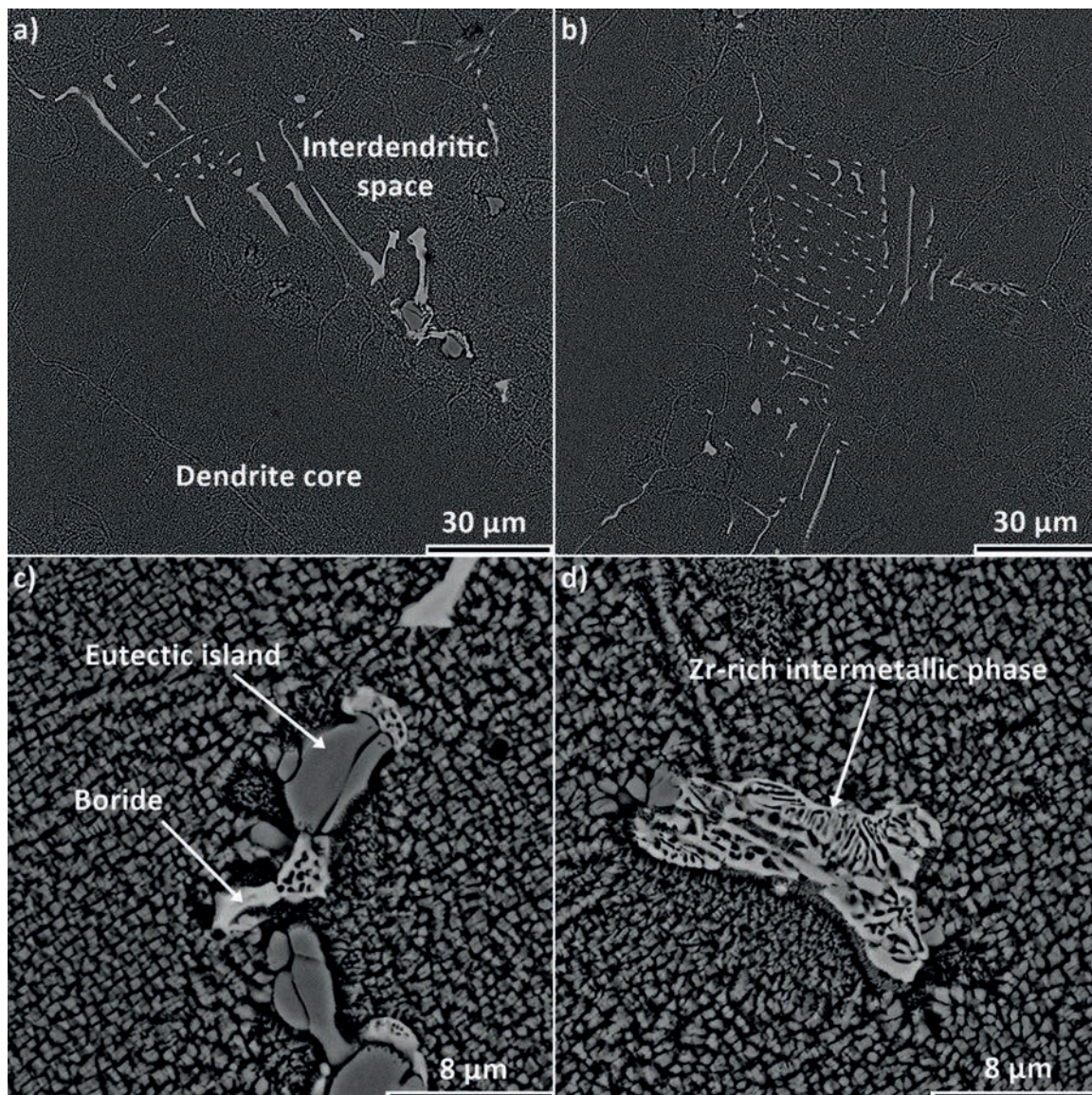
Fig. 5. Microstructure of Inconel 713C before creep test: a) dendrite core and interdendritic space, b) Chinese script carbide, c) eutectic island and boride, d) Zr-rich intermetallic phase
Rys. 5. Mikrostruktura Inconelu 713C przed testem pełzania: a) rdzeń dendrytu i przestrzeń międzydendrytyczna, b) węglik o morfologii chińskiego pisma, c) eutektyka γ/γ' i borek, d) faza międzymetaliczna bogata w cyrkon
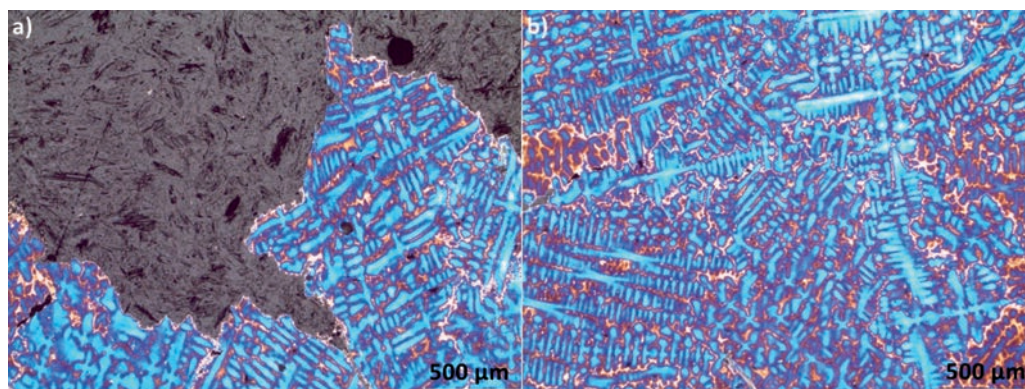

Fig. 6. Microstructure of crept sample: a) fracture, b) small local voids along grain boundaries
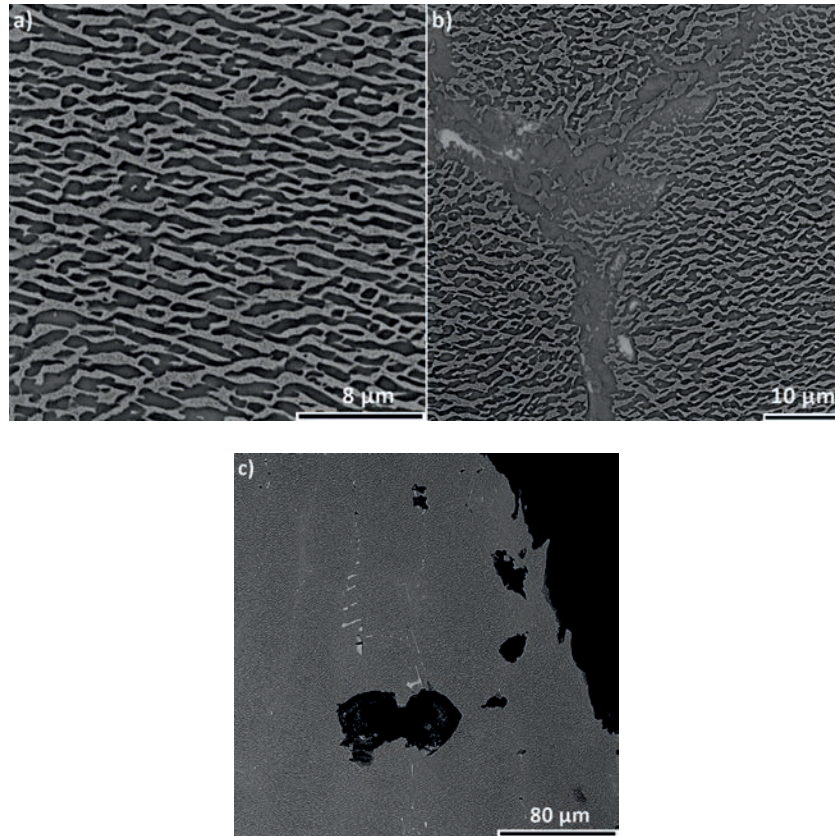*Rys. 6. Mikrostruktura próbki po pełzaniu: a) pęknięcia, b) lokalne pustki wzdłuż granic ziaren*

Fig. 7. Microstructural changes after creep: a) dendrite core, b) interdendritic space, c) voids inside the material
Rys. 7. Zmiany mikrostruktury po pełzaniu: a) rdzeń dendrytu, b) przestrzeń międzydendrytyczna, c) pustki wewnątrz materiału

ability to γ' precipitates to transform into plates under stress at high temperatures [16], rafting, as shown in Figure 7a. Significant microstructural changes resulting from the formation of precipitates was observed along grain boundaries (Fig. 7b). All these small precipitates were surrounded by coarsed precipitates with high angle grain boundaries. Locally, away from the fracture small voids were also detected (Fig. 7c).

In order to characterize and indentify precipitates, a EDS linear analysis was performed. The line scan is shown in Figure 8, and the distribution of the main alloying elements in Figure 9. Small precipitates were strongly enriched in Cr and Mo and a high drop in content occured there for Ni and Al. Coarse precipitates observed in the vicinity of small precipitates were enriched especially in Al. After creep testing, the volume fraction of the MC (Nb-rich) carbides in the interdendritic areas was significantly decreased due to partial dissolution at the high homologous temperature. Usually in Ni-based superalloys most of the carbon below 982°C is in the form of MC-type carbide. During service or testing at elevated temperature, MC decomposes slowly to produce carbon that diffuses and triggers an important reactions The dominating reaction in the superalloys is the formation of $M_{23}C_6$-type carbide by the following reaction [16,17]:
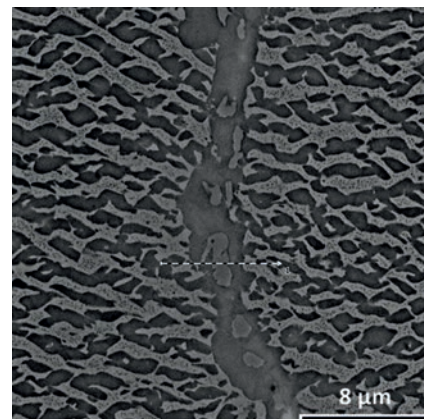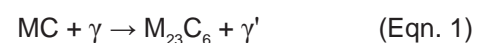

Fig. 8. Location of EDS line scan across grain boundary
Rys. 8. Lokalizacja analizy liniowej EDS wzdłuż granicy ziaren

$$MC + \gamma \rightarrow M_{23}C_6 + \gamma' \qquad \text{(Eqn. 1)}$$

Reaction occurs at about 982°C or even as low as 760°C. Our results indicate that, in accord with Equation 1, small $M_{23}C_6$ carbide particles enriched mainly in Cr and Mo were surrounded by the intermetallic phase γ'.
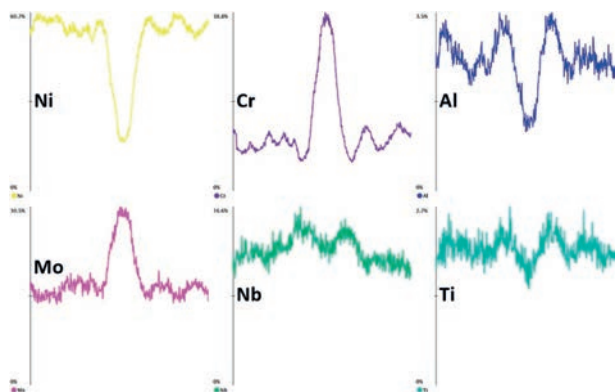
Fig. 9. Distribution of the main alloying elements through grain boundary

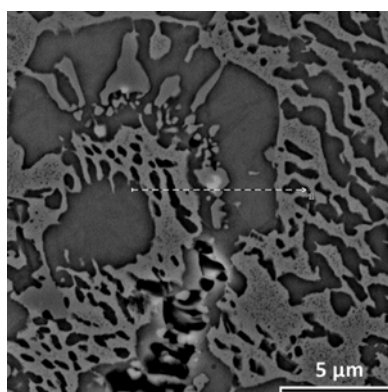*Rys. 9. Rozkład głównych pierwiastków stopowych wzdłuż granicy ziaren*

Fig. 10. Location of EDS line scan in the interdendritic space

Rys. 10. Lokalizacja analizy liniowej EDS w przestrzeni międzydendrytycznej
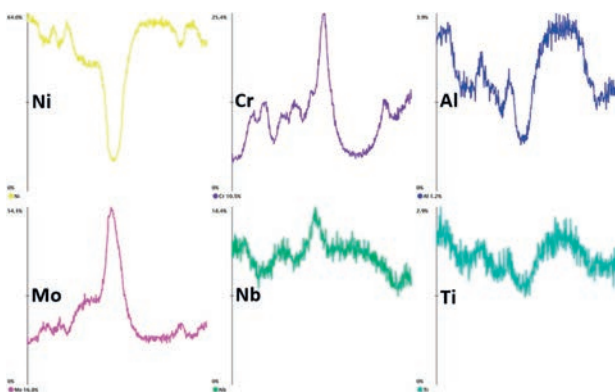

Fig. 11. Distribution of the main alloying elements in interdendritic space

Rys. 11. Rozkład głównych pierwiastków stopowych w przestrzeni międzydendrytycznej

Microstructural changes in the interdendritic space together with the EDS line scan are shown in Figure 10. Large eutectic γ' precipitates did not significantly deform

with the formation of platelet morphology, however, in their close vicinity, the smaller ones underwent such transformation. The results of the EDS analysis shown in Figure 11 indicated a strong enrichment in Cr, Mo and Nb in the area of the bright fine precipitate. The second commonly observed mechanism of MC-type carbide degradation is described by Equation 2 [17]:

$$MC + \gamma \rightarrow M_6C + \gamma' \qquad \text{(Eqn. 2)}$$
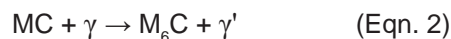
Microstructural degradation of MC carbides led to creation of M_6C-type carbides which are most often rich in Mo, W, Co, Cr and Fe. The presence of these carbides was not detected, despite intensive observations. It was shown that the phase rich in Cr and Mo in the eutectic, was a M_3B_2 boride. The presence of M_3B_2 borides and $M_{23}C_6$ Cr-rich secondary carbides observed after creep can be explained by the low solubility of B and C in the matrix. During exposure to high homologous temperature the MC-type carbides undergo a transformation, and thus, in the regions of their decomposition, the solid solution of matrix becomes enriched with C. Carbon due to larger atomic radius reduces the solubility of B in the matrix and leads to the creation of both borides and secondary carbides at room temperature.

4. Summary

At high temperature/low stress (982°C/152 MPa), Inconel 713C showed short-term primary stage and then steady-state creep (0.057875% per h) and finally pronounced strain appearing at the tertiary stage. The time to rupture was almost 40 h. Microstructure in the as cast condition of Inconel 713C was characterized by dendritic structure with irregular distribution of phases. Dendrite cores consisted of high volume fraction of γ' phase surrounded by channels of the matrix, while segregation of Al, Nb, Zr, and C into interdendritic spaces led to the formation of eutectic islands, carbides, borides and Zr-rich intermetallic phase. Observation of degraded microstructure indicated significant changes that include N-type rafting (directional growth) of γ' precipitates. In interdendritic spaces, including grain boundaries, decomposition of MC-type into $M_{23}C_6$ carbides was observed. Borides enriched in Cr and Mo were also present, so during creep their complete dissolution in the matrix does not occur. Formation of $M_{23}C_6$ carbides can be accompanied by borides formation.

Acknowledgements

References

1. Reed R.C. 2006. *The Superalloys: Fundamentals and Applications*. Cambridge: Cambridge University Press.

2. Benini E. 2011. *Advances in Gas Turbine Technology*. London: IntechOpen.

3. Rakoczy Ł., M. Grudzień, A. Zielińska-Lipiec. 2018. „Contribution of microstructural constituents on hot cracking of MAR-M247 nickel based superalloy". *Archives of Metallurgy and Materials* 63 (1) : 181−189.

4. Rakoczy Ł., M. Grudzień, L. Tuz, K. Pańcikiewicz, A. Zielińska-Lipiec. 2017. „Microstructure and properties of a repair weld in a nickel based superalloy gas turbine component". *Advances in Materials Science* 17 (2) : 55−63.

5. Nguyen L., R. Shi, Y. Wang, M. De Graef. 2016. „Quantification of rafting of γ' precipitates in Ni-based superalloys". *Acta Materialia* 103 (15 January 2016) : 322−333.

6. Nörtershäuser P., J. Frenzel, A. Ludwig, K. Neuking, G. Eggeler. 2015. „The effect of cast microstructure and crystallography on rafting, dislocation plasticity and creep anisotropy of single crystal Ni-base superalloys". *Materials and Engineering: A* 626 (25 February) : 305−312.

7. Cieśla M., F. Binczyk, G. Junak, M. Mańka, P. Gradoń. 2015. „Durability of MAR-247 and IN-713C nickel superalloys under cyclic creep conditions". *Archives of Foundry Engineering* 15 (4) : 17−20.

8. Cieśla M., F. Binczyk, M. Mańka. 2012. „Impact of surface and volume modification of nickel superalloys IN-713C and MAR-247 on high temperature creep resistance". *Archives of Foundry Engineering* 12 (4) : 17−24.

9. Desmorat R., A. Mattiello, J. Cormier. 2017. „A tensorial thermodynamic framework to account for the γ' rafting in nickel-based single crystal superalloys". *International Journal of Plasticity* 95 (August 2017) : 43−81.

10. Touratier F., E. Andrieu, D. Poquillon, B. Viguier. 2009. „Rafting microstructure during creep of the MC2 nickel-based superalloy at very high temperature". *Materials and Engineering: A* 510−511 (15 June 2009) : 244−249.

11. Azadi M., A. Marbout, S. Safarloo, M. Azadi, M. Shariat, M.H. Rizi. 2018. „Effects of solutioning and ageing treatments on properties of Inconel-713C nickel-based superalloy under creep loading". *Materials Science and Engineering: A* 711 (10 January 2018) : 195−204.

12. Matysiak H., M. Zagorska, A. Balkowiec, B. Adamczyk-Cieslak, K. Dobkowski, M. Koralnik, R. Cygan, J. Nawrocki, J. Cwajna, K.J. Kurzydlowski. 2016. „The influence of the melt-pouring temperature and inoculant content on the macro and microstructure of the IN713C Ni-based superalloy". JOM 68 (1) : 185−197.

13. Zupanič F., T. Bončina, A. Križman, F.D. Tichelaar. 2001. „Structure of continuously cast Ni-based superalloy Inconel 713C". *Journal of Alloys and Compounds* 329 (1−2) : 290−297.

14. Standard AMS5391. Nickel Alloy, Corrosion and Heat Resistant, Investment Castings, 73ni 13cr 4.5mo 2.3cb 0.75ti 6.0al 0.010b 0.10zr Vacuum Cast, As-Cast.

15. Cieśla M., F. Binczyk, M. Mańka, R. Findziński. 2014. „The influence of macrostructure of nickel-based superalloys IN713C and MAR 247 on the characteristics of high-temperature creep". *Archives of Foundry Engineering* 14 (4) : 11−16.

16. Matysiak H., M. Zagorska, A. Balkowiec, B. Adamczyk-Cieslak, R. Cygan, J. Cwajna, J. Nawrocki, K.J. Kurzydłowski. 2014. „The microstructure degradation of the IN713C nickel-based superalloy after stress rupture tests". *Journal of Materials Engineering and Performance* 23 (9) : 3305−3013.

17. Bhambri A.K., T.Z. Kattamis, J.E. Morral. 1975. „Cast microstructure of Inconel 713C and its dependence on solidification variables". *Metallurgical Transactions B* 6 (4) : 523−537.